



Fundamental and excitation gaps in molecules of relevance for organic photovoltaics from an optimally tuned range-separated hybrid functional

Sivan Refaely-Abramson,¹ Roi Baer,² and Leeor Kronik¹

¹*Department of Materials and Interfaces, Weizmann Institute of Science, Rehovoth 76100, Israel*

²*Fritz Haber Center for Molecular Dynamics, Institute of Chemistry, Hebrew University, Jerusalem 91904, Israel*

(Received 26 May 2011; published 12 August 2011)

The fundamental and optical gaps of relevant molecular systems are of primary importance for organic-based photovoltaics. Unfortunately, whereas optical gaps are accessible with time-dependent density functional theory (DFT), the highest-occupied – lowest-unoccupied eigenvalue gaps resulting from DFT calculations with semi-local or hybrid functionals routinely and severely underestimate the fundamental gaps of gas-phase organic molecules. Here, we show that a range-separated hybrid functional, optimally tuned so as to obey Koopmans’ theorem, provides fundamental gaps that are very close to benchmark results obtained from many-body perturbation theory in the GW approximation. We then show that using this functional does not compromise the possibility of obtaining reliable optical gaps from time-dependent DFT. We therefore suggest optimally tuned range-separated hybrid functionals as a practical and accurate tool for DFT-based predictions of photovoltaically relevant and other molecular systems.

DOI: [10.1103/PhysRevB.84.075144](https://doi.org/10.1103/PhysRevB.84.075144)

PACS number(s): 71.15.Mb

I. INTRODUCTION

Organic photovoltaics is an emerging technology for the use of sunlight as a clean, renewable energy source.^{1,2} Solar cells based on organic materials are expected to be inexpensive, easy to manufacture, and flexible, allowing for a potentially large assortment of terrestrial applications. Organic photovoltaics is also very interesting from the scientific point of view, because the mechanisms for charge generation, separation, and collection, which control the cell performance, are far from being well understood.³

A key feature of organic semiconductors of the type typically used in solar cells is that their optical absorption is excitonic in nature; i.e., a strongly bound exciton is typically formed upon photon absorption. This bound exciton is subsequently dissociated, usually at an interface between an electron-donating organic semiconductor and an electron accepting one.³ Therefore, from an electronic structure point of view several quantities emerge as crucial for cell performance. For photon absorption, a key quantity is the optical gap, which in the context of organic photovoltaics is defined as the lowest energy required for singlet excitation of the molecule. For charge separation, key quantities are the ionization potential (IP) and electron affinity (EA) of donor and acceptor materials, which control the relative alignment of the various electron and hole levels. The difference between the IP and the EA of a given molecule is typically defined as its fundamental gap.⁴ By definition, the above-defined optical gap differs from the fundamental one by the exciton binding energy, which is often substantial.

Clearly, understanding these properties, and ultimately designing molecules which exhibit desired properties, should be greatly facilitated by theoretical first-principles calculations. Ideally, we would like to use density functional theory (DFT), which allows for the treatment of relatively large systems at a relatively modest computational cost.⁵ For small and medium-size molecules, valence optical excitation energies in general, and optical gaps in particular, are usually

well-predicted by time-dependent DFT (TDDFT) with standard functionals.^{6–11} Unfortunately, it is well-known that with any of the standard exchange-correlation functionals typically employed in a DFT calculation, the highest occupied molecular orbital (HOMO) and the lowest unoccupied molecular orbital (LUMO) are poor predictors for the IP and EA, respectively.⁴ Therefore, other methods, such as coupled-cluster theory¹² or many-body perturbation theory (usually within the GW approximation^{13,14}), are often employed instead, at a greatly increased computational cost.

For Kohn-Sham DFT calculations, i.e., for calculations performed with a local Kohn-Sham potential [e.g., using the local density approximation (LDA)¹⁵ or the general gradient approximation (GGA)¹⁶], the computed HOMO-LUMO gap underestimates the fundamental gap. This is a consequence of the derivative discontinuity problem.^{4,17–19} The Kohn-Sham potential should exhibit a finite “jump” when approaching the integer electron number from below or from above. This discontinuity is essential to capturing the physical discontinuity in the chemical potential, but is not reflected in the Kohn-Sham eigenvalues. DFT calculations with hybrid functionals, which employ a nonlocal potential operator, can partly mitigate the derivative discontinuity problem. However, typical hybrid functionals (such as B3LYP,^{20,21} a popular choice in organic chemistry), which rely on a fraction of exact (Fock) exchange, still greatly underestimate the fundamental gap in finite objects such as molecules. This is because they still lack a correct description of the asymptotic behavior of the exchange-correlation potential.

Range-separated hybrid (RSH) functionals are a relatively new class of functionals that are based on splitting the Coulomb repulsion term into a long-range and a short-range part,^{4,22–25} e.g., via $r^{-1} = r^{-1}\text{erf}(\gamma r) + r^{-1}\text{erfc}(\gamma r)$. The exchange owing to the short-range term is then treated as a local potential, derived for example from standard GGA arguments, whereas the exchange owing to the long-range term is treated via an exact, Fock-like expression. Usually, the

range-separation parameter γ , which provides a characteristic length scale for the transition from the short range to the long range, is determined semi-empirically.^{26–31} This provides a meaningful improvement of fundamental gap prediction, relative to semi-local or standard hybrid functionals, but significant differences with respect to experimental values may still remain.^{27,32}

Recently, we have suggested that excellent fundamental gap values for finite-sized objects may be obtained directly from the HOMO and LUMO eigenvalues if the range-separation parameter γ is optimally tuned rather than semi-empirically fitted.³³ In this approach, the correct γ is determined, per system, by enforcing the DFT version of Koopmans' theorem,^{32,34–36} namely, by insisting that the identity between the HOMO energy and the IP, expected for the exact functional, be obeyed. This approach was already shown to yield excellent results for atoms, a series of oligoacenes, and a series of hydrogenated silicon nanocrystals.³³

A natural question to ask, then, is whether this new approach would also be sufficiently accurate for predicting the IP and the fundamental gap of molecules that are relevant for organic photovoltaics, and furthermore, whether the same framework would still yield useful accuracy for the optical gap, so that it could be used consistently for predicting photovoltaically relevant properties.

Recently, the IP and the HOMO-LUMO gap for a set of organic molecules of photovoltaic interest, shown in Fig. 1, were computed by Blase *et al.*³⁷ using the GW approximation, with good agreement between theory and experiment being obtained throughout. This is a significant achievement, because GW calculations for molecules are difficult, and only a handful of other GW calculations for organic molecules in the gas phase have been reported in the literature,^{38–48} particularly for larger molecules.^{49–54} The set considered by Blase *et al.* serves as an excellent benchmark against which to test the concept of the optimally tuned range-separated hybrid functional approach, for two reasons. The obvious one is its relevance for photovoltaics. A more subtle one is that the molecules in Fig. 1 are not a series in the chemical sense and are related to each other only via a common application. Therefore, a strong demand of equal accuracy across chemically different species is placed on the computational approach.

Here, we show that with the optimally tuned range-separated hybrid functional approach, it is indeed possible to obtain results for the IP and the fundamental gap that are as accurate as GW results. We further show that by employing the same approach within TDDFT, optical gaps that are, on average, as accurate as those obtained by other TDDFT methods are also obtained. This provides a consistent framework for first-principles prediction of fundamental and optical gaps of gas-phase objects at a minimal computational cost.

II. COMPUTATIONAL APPROACH

All range-separated hybrid (RSH) functional calculations presented in this work were performed using the Baer,

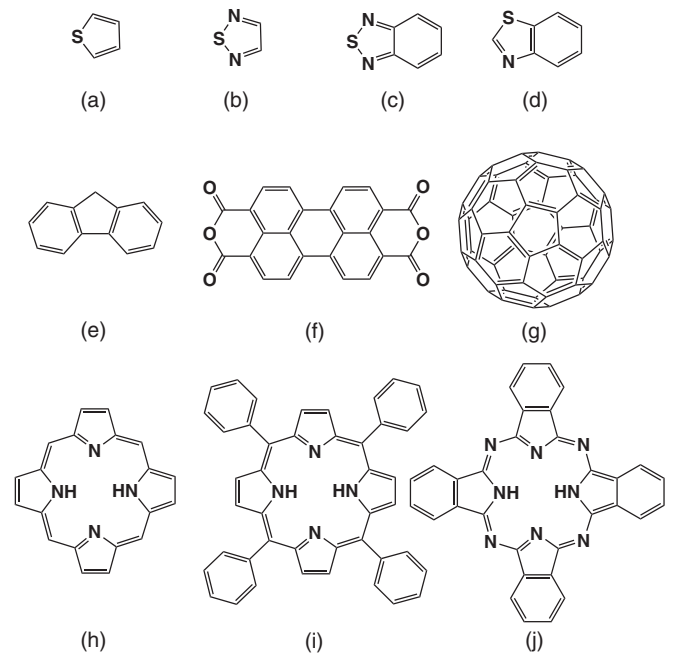


FIG. 1. The set of photovoltaically relevant molecules considered in this work: (a) thiophene, (b) 1,2,5-thiadiazole, (c) 2,1,3-benzothiadiazole, (d) benzothiazole, (e) fluorene, (f) 3,4,9,10-perylene tetracarboxylic acid dianhydride (PTCDA), (g) buckminsterfullerene (C_{60}), (h) 21H,23H-porphine (H_2P), (i) tetraphenylporphyrin (H_2TPP), and (j) phthalocyanine (H_2Pc).

Neuhauser, and Livshits (BNL) RSH functional.²⁶ In this RSH functional, the long-range exchange is given by

$$E_X^\gamma[\{\phi_j\}] = -\frac{1}{2} \sum_{\sigma=\uparrow,\downarrow} \sum_{i,j=1}^{N_\sigma} \iint \phi_{i,\sigma}^*(r) \phi_{j,\sigma}^*(r') \times u_\gamma(|r-r'|) \phi_{j,\sigma}(r) \phi_{i,\sigma}(r') d^3r' d^3r, \quad (1)$$

where $u_\gamma(r) = \text{erf}(\gamma r)/r$ is the long-range two-body interaction. The short-range exchange is given by Savin's local expression,²² derived from the $\text{erfc}(\gamma r)/r$ short-range two-body interaction, and the correlation is the GGA-type Lee-Yang-Parr (LYP) functional.⁵⁵

As discussed above, key to obtaining quantitatively useful results is the correct choice of the range-separation parameter γ , which appears in both the long- and short-range exchange expressions. In order to obtain the correct ionization potential, one should seek γ such that Koopmans' theorem is obeyed as closely as possible; i.e., the target function

$$J(\gamma) = |\varepsilon_H^\gamma(N) + \text{IP}^\gamma(N)| \quad (2)$$

is minimized. In Eq. (2), $\varepsilon_H^\gamma(N)$ is the HOMO energy of the neutral molecule, and $\text{IP}^\gamma(N)$ is the ionization potential of it, calculated from energy differences of the neutral molecule and cation. Here, the superscript γ signifies that both the HOMO energy and the ionization potential depend on the choice of the range-separation parameter. Therefore, the physical content of Eq. (2) is that we seek the value of the range-separation parameter such that the ionization potential, evaluated using this parameter in two different ways—from

the leading eigenvalue or from a total energy difference—will yield the same result.

Because we also wish to obtain the electron affinity, and because a corresponding theorem for EA does not exist, we instead demand that Koopmans' theorem also be obeyed for the IP of the anion, which (barring geometrical relaxation which we do not allow) is the same as the EA of the neutral. Because we now have two conditions but only one parameter, γ , we minimize the following target function:

$$J(\gamma) = |\varepsilon_H^\gamma(N) + \text{IP}^\gamma(N)| + |\varepsilon_H^\gamma(N+1) + \text{IP}^\gamma(N+1)|, \quad (3)$$

where $\varepsilon_H^\gamma(N+1)$ is the HOMO energy of the anion, and $\text{IP}^\gamma(N+1)$ is its ionization potential.

The electronic structure and optical excitation energies for all molecules in Fig. 1 were calculated using DFT and linear-response TDDFT, respectively, using QCHEM 3.2,⁵⁶ which includes the BNL functional. For TDDFT, this involves a straightforward extension of the linear-response formalism from a conventional hybrid functional to an RSH one, as shown, e.g., in Ref. 57. The correlation-consistent polarized valence triple zeta (cc-pVTZ) basis set was used throughout, with the double zeta (cc-PVDZ) used to assess convergence.⁵⁸ For facilitating the comparison with the results of Blase *et al.*,³⁷ we have used their LDA-based geometries. Additionally, we tested that use of these geometries within our computational framework does not result in significant forces. All fundamental- and optical-gap predictions from BNL calculations were based solely on the optimal choice of γ . The optimal value was found using Eq. (3), unless the molecule did not possess a positive EA, in which case Eq. (2) was used. For comparison, B3LYP-based computations for the same quantities were also performed.

III. RESULTS

A. Tuning γ

The optimally tuned range-separation parameter γ for each molecule is given in tabular form in Table I and in graphical form in Fig. 2, as a function of the molecules' characteristic radius. Here and throughout, γ is given in atomic units, namely, bohr⁻¹. The radius was determined by the standard deviation of the atoms from the center of the molecule. It is readily observed that no single value of γ is universally optimal. As a guideline, optimal γ values decrease with increasing molecular size. However, the dependence is not monotonic and also depends on the specific chemical nature of the molecule.

B. Ionization potentials

The ionization potentials predicted from the eigenvalue corresponding to the HOMO, from both optimally tuned BNL and B3LYP, are given in Table II, where they are additionally compared to experimental results and to the (eigenvalue self-consistent) GW results of Ref. 37. The same data are presented in graphical form in Fig. 3.

As expected, the B3LYP eigenvalues significantly and consistently underestimate the experimental values, with an unsatisfactory average error of 1.76 eV. The GW results also

TABLE I. Optimally tuned values of the range parameter γ (in atomic units) and characteristic radii (in Å) for the molecules shown in Fig. 1. The radii were determined from the standard deviation of the atoms from the average of the molecular coordinates.

Molecule	Optimal γ	Characteristic Radius (Å)
(a) thiophene	0.313	1.83
(b) thiadiazole	0.355	1.54
(c) benzothiadiazole	0.288	2.22
(d) benzothiazole	0.293	2.41
(e) fluorene	0.240	3.07
(f) PTCDA	0.207	4.07
(g) C ₆₀	0.211	3.55
(h) H ₂ P	0.252	3.97
(i) H ₂ TPP	0.152	5.77
(j) H ₂ Pc	0.162	5.29

underestimate the experimental data, but by a much smaller average error of 0.30 eV. The optimally tuned BNL eigenvalues sometimes underestimate and sometimes overestimate the experimental data, with average signed and unsigned errors of only 0.02 eV and 0.12 eV, respectively. To examine the influence of the range parameter on the results, we calculated the ionization potential taking a fixed value of $\gamma = 0.25$. The resulting IP values for this γ had a larger unsigned error of 0.20 eV from experiment.

C. HOMO-LUMO gaps

The HOMO-LUMO gaps predicted from the difference between the eigenvalues corresponding to the HOMO and the LUMO, from both optimally tuned BNL and B3LYP, are given in Table III, where they are also compared to the (eigenvalue self-consistent) GW results of Ref. 37. Because experimental

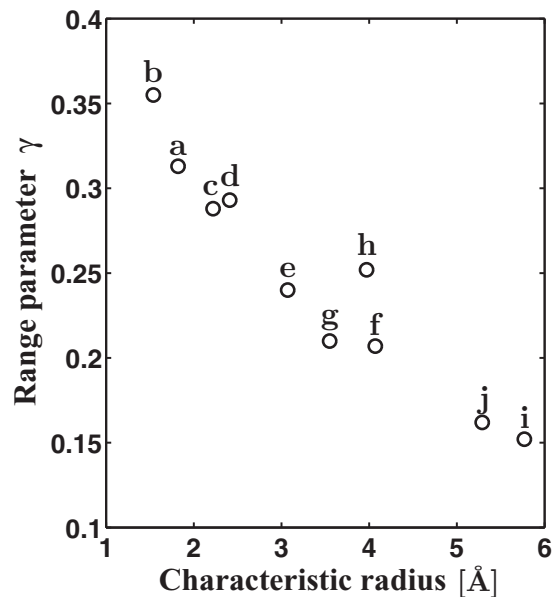


FIG. 2. Graphical representation of the data in Table I: Optimally tuned values of the range parameter γ (in atomic units) for the molecules shown in Fig. 1, as a function of the molecular characteristic radius (in Å).

TABLE II. Ionization potentials, in eV, for the molecules of Fig. 1. EXP: Experimental values, adapted from (i) Ref. 59, (ii) Ref. 60, (iii) Ref. 49, (iv) Ref. 54, and (v) Ref. 61. OT-BNL: HOMO eigenvalue of an optimally tuned BNL calculation. GW: Many-body perturbation theory results from Ref. 37. B3LYP: HOMO eigenvalue of a B3LYP calculation.

Molecule	EXP	OT-BNL	GW	B3LYP
(a) thiophene	8.89 ⁱ	9.01	8.63	6.56
(b) thiadiazole	10.11 ⁱⁱ	10.26	9.89	7.70
(c) benzothiadiazole	8.99 ⁱ	8.98	8.56	6.83
(d) benzothiazole	8.74 ⁱ	8.84	8.48	6.67
(e) fluorene	8.03 ⁱ	7.89	7.64	6.01
(f) PTCDA	8.20 ⁱⁱⁱ	8.08	7.68	6.67
(g) C ₆₀	7.64 ⁱ	7.89	7.41	6.29
(h) H ₂ P	6.90 ⁱ	6.97	6.70	5.47
(i) H ₂ TPP	6.37 ^{i,iv}	6.26	6.20	5.25
(j) H ₂ Pc	6.41 ^v	6.31	6.10	5.20

electron affinities of the molecules in Fig. 1 are harder to obtain, we only present experimental reference values for two of the molecules. For molecules with negative electron affinity, we used only the IP for the γ tuning [Eq. (2)], as explained above. The same data are presented graphically in Fig. 4.

The B3LYP fundamental gaps are smaller than the reference GW gaps, with an average error of 3.25 eV. The optimally tuned BNL fundamental gaps sometimes underestimate and sometimes overestimate the reference GW values, with average signed and unsigned errors of 0.10 eV and 0.19 eV, respectively. To examine the influence of the range parameter on the results, we also calculated the fundamental gap taking a fixed value of $\gamma = 0.25$. The resulting HOMO-LUMO gap for

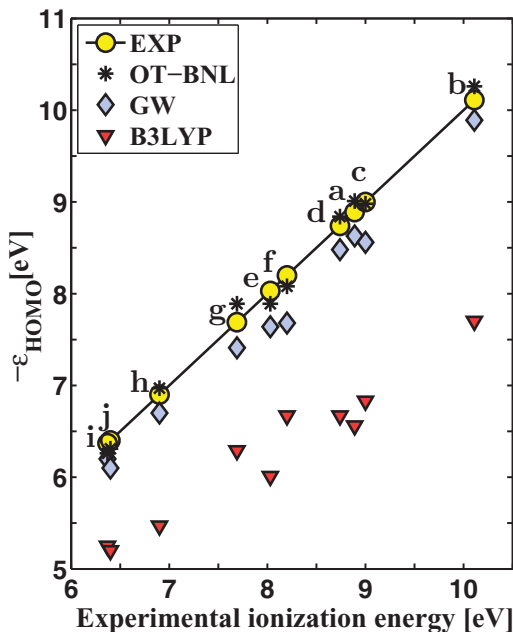


FIG. 3. (Color online) Graphical representation of the data in Table II for the ionization potentials of the molecules in Fig. 1. Yellow circles, experimental values; stars, optimally tuned BNL values; blue diamonds, GW values; red triangles, B3LYP values.

TABLE III. HOMO-LUMO gaps, in eV, for the molecules of Fig. 1. EXP: Experimental values, adapted from (i) Ref. 59 and (ii) Ref. 62. OT-BNL: The difference between the LUMO and the HOMO eigenvalues of an optimally tuned BNL calculation. GW: Many-body perturbation theory results from Ref. 37. B3LYP: The difference between the LUMO and the HOMO eigenvalues of a B3LYP calculation.

Molecule	EXP	OT-BNL	GW	B3LYP
(a) thiophene		10.45	10.61	5.90
(b) thiadiazole		10.56	10.81	5.74
(c) benzothiadiazole		8.16	8.14	4.16
(d) benzothiazole		9.36	9.40	5.28
(e) fluorene		8.38	8.38	4.84
(f) PTCDA		5.25	5.00	2.50
(g) C ₆₀	4.96 ⁱ	5.47	4.91	2.59
(h) H ₂ P		5.66	5.31	2.88
(i) H ₂ TPP	4.65 ^{i,ii}	4.82	4.71	2.75
(j) H ₂ Pc		4.24	4.03	2.10

this γ has a significantly larger unsigned error of 0.59 eV from the GW reference values, with the largest error being 1.1 eV, obtained for C₆₀.

For four of the molecules—thiophene, thiadiazole, benzothiazole, and fluorene—the LUMO level obtained from the BNL calculation is positive, suggesting a negative EA. Correspondingly, for these molecules the fundamental gap predicted from the calculation is larger than the IP. The same phenomenon was encountered in the reference GW calculations. Conversely, the B3LYP eigenvalues would imply positive EA for those molecules. Here, it is important to note that, strictly speaking, for a “negative EA” we would expect $\epsilon_{\text{LUMO}} = 0$, obtained at the limit of infinite separation between

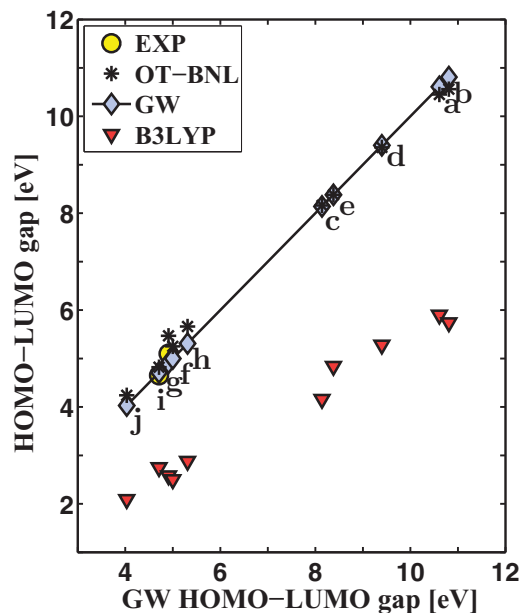


FIG. 4. (Color online) Graphical representation of the data in Table III for the HOMO-LUMO gaps of the molecules in Fig. 1. Yellow circles, experimental values; stars, optimally tuned BNL values; blue diamonds, GW values; red triangles, B3LYP values.

TABLE IV. First singlet excitation, in eV, for the molecules in Fig. 1. EXP: Experimental values, adapted from (i) Ref. 67, (ii) Ref. 68, (iii) Ref. 69, (iv) Ref. 70, (v) Ref. 71, (vi) Ref. 72, (vii) Ref. 73, and (viii) Ref. 74. OT-BNL: First singlet excitation of an optimally tuned BNL TDDFT calculation. B3LYP: First singlet excitation of a B3LYP TDDFT calculation.

Molecule	EXP	OT-BNL	B3LYP
(a) thiophene	5.52 ⁱ	5.79	5.75
(b) thiadiazole	5.00 ⁱⁱ	5.22	5.05
(c) benzothiadiazole	4.05 ⁱⁱⁱ	4.15	3.71
(d) benzothiazole	n/a	4.81	4.61
(e) fluorene	4.19 ^{iv}	4.65	4.43
(f) PTCDA	2.60 ^v	2.58	2.41
(g) C ₆₀	2.24 ^{vi}	2.32	1.96
(h) H ₂ P	2.16 ^{vii}	2.07	2.26
(i) H ₂ TPP	2.06 ^{viii}	2.09	2.16
(j) H ₂ Pc	1.81 ^{viii}	1.97	2.01

the extra electron and molecule. However, this limit cannot be obtained in either the BNL or the GW calculations due to the finite basis set.^{63–65} We return to this issue in the discussion below, but point out that in any case the performance of the optimally tuned BNL approach still matches that of the GW one.

D. Optical gaps

The optical gaps predicted from the lowest energy required for singlet excitation, from both optimally tuned BNL and B3LYP, are given in Table IV, where they are additionally compared to the experimental values (except for benzothiazole, for which we are unaware of an experimental value). In principle, it is possible to obtain optical gap values within many-body perturbation theory by combining the GW method with the Bethe-Salpeter equation (BSE).⁶⁶ However, we are only aware of such results for H₂P and H₂TPP,⁵² where in both cases the BSE values are in a good agreement with our results, and for C₆₀,⁵⁰ where the BNL result is in better agreement with gas phase optical data.⁷² The data are also presented in graphical form in Fig. 5.

As expected, and consistent with previous work,⁹ the B3LYP values for the optical gaps are close to the experimental values, with an average signed and unsigned errors of 0.01 eV and 0.19 eV, respectively. The optimally tuned BNL values are also close to experiment, with an average signed and unsigned error of 0.14 eV and 0.16 eV, respectively. Furthermore, the BNL and B3LYP values are as close to each other as they are close to experiment, with a signed and unsigned relative error between the two theories of 0.12 eV and 0.19 eV, respectively.

IV. DISCUSSION

In the preceding section, we have explored the fundamental and optical gaps resulting from an optimally tuned BNL calculation of a set of organic molecules relevant for photovoltaic applications. The optimally tuned BNL results for the ionization potential are in very good agreement with

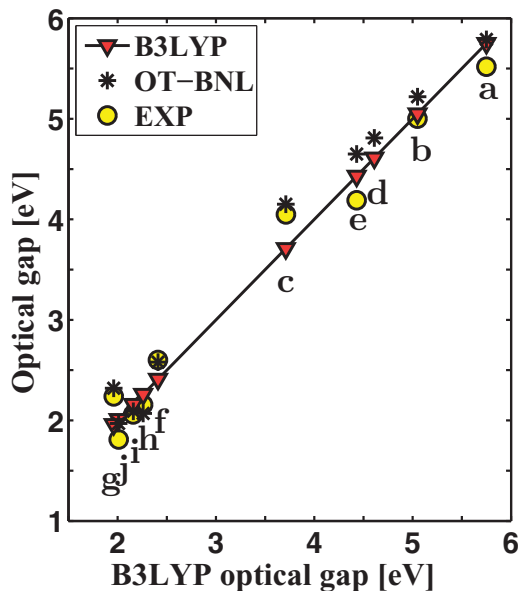


FIG. 5. (Color online) Graphical representation of the data in Table IV for the first singlet excitation energies of the molecules in Fig. 1. Red triangles, B3LYP values; stars, optimally tuned BNL values; yellow circles, experimental values.

experiment, differing from it by an average unsigned error of only 0.12 eV. In comparison, the average deviation of the reference GW sequence is 0.30 eV. This implies that optimally tuned BNL is appropriate for reliable and computationally inexpensive ionization potential calculations of gas-phase organic molecules.

The optimally tuned BNL results for the electron affinity are also satisfying, due to the minimization of the derivative discontinuity, as explained above. Compared to reference GW values, for lack of experimental values, the resulting HOMO-LUMO gap average unsigned error from the GW results is only 0.19 eV, which is within the accepted error for both the BNL and the GW calculations. The largest deviation found (for C₆₀, with respect to experiment) was 0.37 eV—a slightly larger, but still tolerable, error.

The electron affinity of thiophene, thiadiazole, benzothiazole, and fluorene (obtained from total energy differences) is negative, in agreement with the GW results. Tozer and de Prof⁶⁴ suggested that for molecules with negative electron affinity, medium-sized basis set DFT calculations on the anion can give energies above that of the neutral molecule. The total energy difference between neutral and anion can then serve as a reasonable estimation for the negative affinity that can be obtained experimentally by probing resonant states. This success is due to the artificial binding of the electron by the finite basis set.^{63–65} For the above four molecules, we find that the LUMO eigenvalues obtained from the optimally tuned BNL calculations are positive, corresponding to a negative electron affinity. Furthermore, the LUMO eigenvalues are very close to the reference electron affinity values obtained from GW (calculating the same quantities with the cc-pVDZ basis set led to similar results). Possibly, this is because the BNL and GW calculations probe similar resonance values. Alternatively, it is because both the BNL and the GW calculations artificially “bind” the LUMO orbital, albeit in

different ways. In BNL, this is due to the finite basis set. In GW, it is because the quasiparticle orbitals are obtained from LDA, for which the LUMO can still be bound owing to the small HOMO-LUMO gap.³⁸ In either case, it is interesting that the optimally tuned BNL functional has the ability of imitating the quasiparticle nature of a GW calculation even in this “difficult case.”

The optimally tuned BNL results for the optical gap are as close to the B3LYP values as they are to the experimental ones, with an average unsigned error of 0.19 eV and 0.16 eV, respectively. B3LYP-based TDDFT calculations for organic molecules usually result in reliable optical gap values. Hence, the resulting optimally tuned BNL optical gap values are satisfying. Furthermore, it is reasonable to assume that for systems that contain such molecules, the results would be even better than those obtained with B3LYP. This is because the optimally tuned RSH functional approach would still perform satisfactorily where B3LYP fails, e.g., for charge transfer situations.^{75–77} This is further illustrated by the benzothiadiazole example. There, the B3LYP excitation energy underestimates experiment by 0.34 eV, whereas the optimally tuned BNL is only 0.10 eV away from experiment. A possible explanation is that this is a charge-transfer-like phenomenon, recently described in the context of polyaromatic hydrocarbons.⁵⁷ In such excitations, charge-transfer behavior is not observed for the original orbitals but becomes apparent in auxiliary orbitals obtained from a unitary transformation, and therefore the correct long-range asymptotic behavior can be as important as it is in true charge transfer scenarios. The optimally tuned BNL functional therefore provides a consistent, reliable, and low-cost framework for the prediction of both the fundamental and the optical gaps of gas-phase molecules.

The high accuracy of the optimally tuned BNL functional is due to a combination of two important principles. The first is the use of a generalized Kohn-Sham (GKS) scheme^{4,78,79} with the correct long-range asymptotic behavior. Within the GKS scheme, the interacting electron system is mapped into an interacting model system that can still be represented by a single Slater determinant. This leads to a nonlocal, orbital-specific operator accompanied by a “remainder” local potential. The nonlocal operator inherently exhibits discontinuity as the particle number crosses an integer due to partial occupation of an additional orbital; hence it can greatly diminish the derivative discontinuity in the potential and can result in fundamental gaps that are much closer to experiment than the Kohn-Sham gap.^{4,32,33,78} In this respect, standard hybrid functionals can also be considered as special cases of a GKS scheme.^{4,79} However, because standard hybrid functionals only incorporate a fraction of exact exchange, they still do not possess the correct long-range asymptotic behavior of the potential, which is crucial for a correct description of electron removal or insertion processes. RSH functionals with asymptotically exact exchange, such as the BNL functional used here, do possess the correct asymptotic behavior by construction^{33,79} and are therefore a much better choice *a priori*.

The second principle behind the success of our results is the system-dependent range-parameter tuning. While RSH functionals can yield the correct results, success in practice requires that the correct balance between the short- and

long-range exchange be maintained. It is well demonstrated in our results that the range-parameter γ tuning procedure is significant in that respect. First, a clear molecular dependence of the optimal γ value is observed, as it generally decreases with the molecular size. A similar trend has been previously noted for Si nanocrystals and oligoacenes³³ and can be explained similarly: The electron delocalization increases with molecule size, resulting in a smaller needed weight of exact exchange. Alternatively, one can view γ^{-1} as an effective screening length, with screening being generally more efficient with increasing system size. This view is consistent with the correlation between γ^{-1} and the optical dielectric constant, found if one fits the range-separation parameter so as to obtain the experimental band gap in solids.⁸⁰ However, we note that the size-dependence of γ^{-1} is a guideline only, because delocalization and screening clearly depend on the system details. For example, the optimal γ for H₂P is slightly larger than that expected from the scaling curve of the other molecules. As further demonstration of the importance of tuning, consider fixing the range-separation parameter to a constant “compromise value” of 0.25. Additional calculations with this fixed value indicate that the average unsigned error, with respect to experiment, of the IP increases only slightly—from 0.12 eV in the optimally tuned systems to 0.20 eV in the nontuned systems. However, for the resulting HOMO-LUMO gap, the average unsigned error from the reference values changes significantly: from 0.19 eV in the optimally tuned systems to 0.59 eV in the nontuned ones. This immediately explains the fundamental difficulty in using RSH functionals that contain a fixed value of γ , and the importance of a system-dependent tuning procedure.

V. CONCLUSIONS

We have explored the fundamental and optical gaps of a set of organic molecules of photovoltaic interest with the optimally tuned BNL range-separated hybrid functional. Our results for the ionization potentials and the HOMO-LUMO gaps are very close to GW results, and to experimental values where such exist. The results for the optical gaps are close to B3LYP values and to experiment. We therefore conclude that the optimally tuned BNL functional is an appropriate tool for calculations of fundamental and optical gaps of organic gas-phase molecules. Because the GW approach may be computationally expensive for large systems, DFT calculations based on the optimally tuned BNL functional emerge as a highly promising method for such calculations.

ACKNOWLEDGMENTS

We gratefully thank Xavier Blase (Institut Néel, CNRS, and Université Joseph Fourier, Grenoble) for helpful discussions and for providing molecular coordinates. We also thank Sanford Ruhman (Hebrew University), Tamar Stein (Hebrew University), and Natalia Kuritz (Weizmann Institute) for illuminating discussions. Work in Rehovoth was supported by the Israel Science Foundation and the Lise Meitner Minerva Center for Computational Chemistry. Work in Jerusalem was supported by the US-Israel Binational Science Foundation.

- ¹J. J. M. Halls and R. H. Friend, in *Clean Electricity from Photovoltaics*, edited by M. D. Archer and R. Hill (Imperial College Press, London, 2001), Chap. 9, pp. 377–446.
- ²C. J. Bradec, V. Dyakonov, J. Parisi, and N. S. Sariciftci, eds., *Organic Photovoltaics: Concepts and Realization* (Springer Series in Materials Science, Berlin, 2003).
- ³J. L. Brédas, J. E. Norton, J. Cornil, and V. Coropceanu, *Acc. Chem. Res.* **42**, 1691 (2009).
- ⁴S. Kümmel and L. Kronik, *Rev. Mod. Phys.* **80**, 3 (2008).
- ⁵W. Koch and M. Holthausen, *A Chemist's Guide to Density Functional Theory*, 2nd ed. (Wiley-VCH, Weinheim, 2000).
- ⁶M. A. L. Marques, A. Rubio, C. A. Ullrich, K. Burke, F. Nogueira, and E. K. U. Gross, eds., *Time-Dependent Density Functional Theory* (Springer, Berlin, 2006).
- ⁷K. Burke, J. Werschnik, and E. K. U. Gross, *J. Chem. Phys.* **123**, 062206 (2005).
- ⁸J. R. Chelikowsky, L. Kronik, and I. Vasiliev, *J. Phys. Condens. Matter* **15**, R1517 (2003).
- ⁹M. R. Silva, M. Schreiber, S. P. A. Sauer, and W. Thiel, *J. Chem. Phys.* **129**, 104103 (2008).
- ¹⁰C. Adamo, G. E. Scuseria, and V. Barone, *J. Chem. Phys.* **111**, 2889 (1999).
- ¹¹F. Furche and R. Ahlrichs, *J. Chem. Phys.* **117**, 7433 (2002).
- ¹²I. Shavitt and J. Bartlett, *Many-Body Methods in Chemistry and Physics: MBPT and Coupled-Cluster Theory* (Cambridge University Press, New York, 2009).
- ¹³L. Hedin, *Phys. Rev.* **139**, A796 (1965).
- ¹⁴M. S. Hybertsen and S. G. Louie, *Phys. Rev. B* **34**, 5390 (1986).
- ¹⁵W. Kohn and L. J. Sham, *Phys. Rev.* **140**, A1133 (1965).
- ¹⁶J. P. Perdew and S. Kurth, in *A Primer in Density Functional Theory*, edited by C. Fiolhais, F. Nogueira, and M. Marques (Springer, Berlin, 2003), Chap. 1, pp. 1–55.
- ¹⁷J. P. Perdew and M. Levy, *Phys. Rev. Lett.* **51**, 1884 (1983); L. J. Sham and M. Schlüter, *Phys. Rev. Lett.* **84**, 1888 (1983).
- ¹⁸R. W. Godby, M. Schlüter, and L. J. Sham, *Phys. Rev. Lett.* **56**, 2415 (1986).
- ¹⁹M. J. Allen and D. J. Tozer, *Mol. Phys.* **100**, 433 (2002).
- ²⁰A. D. Becke, *J. Chem. Phys.* **98**, 1372 (1993).
- ²¹P. J. Stephens, F. J. Devlin, C. F. Chabalowski, and M. J. Frisch, *J. Phys. Chem.* **98**, 11623 (1994).
- ²²J. Toulouse, A. Savin, and H. J. Flad, *Int. J. Quantum Chem.* **100**, 1047 (2004).
- ²³T. Leininger, H. Stoll, H. J. Werner, and A. Savin, *Chem. Phys. Lett.* **275**, 151 (1997).
- ²⁴R. Baer and D. Neuhauser, *Phys. Rev. Lett.* **94**, 043002 (2005).
- ²⁵Y. Tawada, T. Tsuneda, S. Yanagisawa, T. Yanai, and K. Hirao, *J. Chem. Phys.* **120**, 8425 (2004).
- ²⁶E. Livshits and R. Baer, *Phys. Chem. Chem. Phys.* **9**, 2932 (2007).
- ²⁷J. D. Chai and M. Head-Gordon, *J. Chem. Phys.* **128**, 084106 (2008).
- ²⁸O. A. Vydrov and G. E. Scuseria, *J. Chem. Phys.* **125**, 234109 (2006).
- ²⁹A. J. Cohen, P. Mori-Sánchez, and W. T. Yang, *J. Chem. Phys.* **126**, 191109 (2007).
- ³⁰B. M. Wong and J. G. Cordaro, *J. Chem. Phys.* **129**, 214703 (2008).
- ³¹M. A. Rohrdanz, K. M. Martins, and J. M. Herbert, *J. Chem. Phys.* **130**, 054112 (2009).
- ³²A. J. Cohen, P. Mori-Sánchez, and W. T. Yang, *Phys. Rev. B* **77**, 115123 (2008).
- ³³T. Stein, H. Eisenberg, L. Kronik, and R. Baer, *Phys. Rev. Lett.* **105**, 266802 (2010).
- ³⁴J. P. Perdew, R. G. Parr, M. Levy, and J. J. L. Balduz, *Phys. Rev. Lett.* **49**, 1691 (1982).
- ³⁵C. O. Almbladh and U. von Barth, *Phys. Rev. B* **31**, 3231 (1985).
- ³⁶U. Salzner and R. Baer, *J. Chem. Phys.* **131**, 231101 (2009).
- ³⁷X. Blase, C. Attaccalite, and V. Olevano, *Phys. Rev. B* **83**, 115103 (2011).
- ³⁸J. C. Grossman, M. Rohlfing, L. Mitas, S. G. Louie, and M. L. Cohen, *Phys. Rev. Lett.* **86**, 472 (2001).
- ³⁹S. Ismail-Beigi and S. G. Louie, *Phys. Rev. Lett.* **90**, 076401 (2003); K. Ohno, S. Ishii, and Y. Noguchi, *J. Phys.: Conf. Ser.* **29**, 39 (2006).
- ⁴⁰M. L. Tiago and J. R. Chelikowsky, *Solid State Commun.* **136**, 333 (2005).
- ⁴¹M. L. Tiago and J. R. Chelikowsky, *Phys. Rev. B* **73**, 205334 (2006).
- ⁴²J. B. Neaton, M. S. Hybertsen, and S. G. Louie, *Phys. Rev. Lett.* **97**, 216405 (2006).
- ⁴³P. Umari, G. Stenuit, and S. Baroni, *Phys. Rev. B* **79**, 201104 (2009).
- ⁴⁴Y. C. Ma, M. Rohlfing, and C. Molteni, *Phys. Rev. B* **80**, 241405 (2009).
- ⁴⁵C. Rostgaard, K. W. Jacobsen, and K. S. Thygesen, *Phys. Rev. B* **81**, 085103 (2010).
- ⁴⁶P. Umari, C. Castellarin-Cudia, V. Feyer, G. Di Santo, P. Borghetti, L. Sangaletti, G. Stenuit, and A. Goldoni, *Phys. Status Solidi B* **248**, 960 (2011).
- ⁴⁷C. Faber, C. Attaccalite, V. Olevano, E. Runge, and X. Blase, *Phys. Rev. B* **83**, 115123 (2011).
- ⁴⁸J. M. Garcia-Lastra and K. S. Thygesen, *Phys. Rev. Lett.* **106**, 187402 (2011).
- ⁴⁹N. Dori, M. Menon, L. Kilian, M. Sokolowski, L. Kronik, and E. Umbach, *Phys. Rev. B* **73**, 195208 (2006).
- ⁵⁰M. L. Tiago, P. R. C. Kent, R. Q. Hood, and F. A. Reboredo, *J. Chem. Phys.* **129**, 084311 (2008).
- ⁵¹L. G. G. V. Dias da Silva, M. L. Tiago, S. E. Ulloa, F. A. Reboredo, and E. Dagotto, *Phys. Rev. B* **80**, 155443 (2009).
- ⁵²M. Palummo, C. Hogan, F. Sottile, P. Bagalá, and A. Rubio, *J. Chem. Phys.* **131**, 084102 (2009).
- ⁵³P. Umari, G. Stenuit, and S. Baroni, *Phys. Rev. B* **81**, 115104 (2010).
- ⁵⁴G. Stenuit, C. Castellarin-Cudia, O. Plekan, V. Feyer, K. C. Prince, A. Goldoni, and P. Umari, *Phys. Chem. Chem. Phys.* **12**, 10812 (2010).
- ⁵⁵C. T. Lee, W. T. Yang, and R. G. Parr, *Phys. Rev. B* **37**, 785 (1988).
- ⁵⁶Y. Shao, L. F. Molnar, Y. Jung, et al., *Phys. Chem. Chem. Phys.* **8**, 3172 (2006).
- ⁵⁷N. Kuritz, T. Stein, R. Baer, and L. Kronik, *J. Chem. Theory Comput.* **7**, 2408 (2011).
- ⁵⁸T. H. Dunning, *J. Chem. Phys.* **90**, 1007 (1989).
- ⁵⁹Data are taken from the National Institute of Standards and Technology web book at [<http://webbook.nist.gov>]. The given values are the averages of the different experimental gas-phase vertical ionization potentials and electron affinities reported in the web book.
- ⁶⁰T. Pasinszki, M. Krebsz, and G. Vass, *J. Mol. Struct.* **966**, 85 (2010).
- ⁶¹J. Berkowitz, *J. Chem. Phys.* **70**, 2819 (1979).
- ⁶²H. L. Chen, Y. H. Pan, S. Groh, T. E. Hagan, and D. P. Ridge, *J. Am. Chem. Soc.* **113**, 2766 (1991).
- ⁶³N. Rösch and S. B. Trickey, *J. Chem. Phys.* **106**, 8940 (1997).
- ⁶⁴D. J. Tozer and F. de Proft, *J. Phys. Chem. A* **109**, 8923 (2005).
- ⁶⁵O. Guliamov, L. Kronik, and J. M. L. Martin, *J. Phys. Chem. A* **111**, 2028 (2007).

- ⁶⁶M. Rohlfing and S. G. Louie, *Phys. Rev. Lett.* **80**, 3320 (1998).
- ⁶⁷M. H. Palmer, I. C. Walker, and M. F. Guest, *Chem. Phys.* **241**, 275 (1999).
- ⁶⁸M. H. Palmer, *Chem. Phys.* **348**, 130 (2008).
- ⁶⁹J. M. Hollas and R. A. Wright, *Spectrochim. Acta, Part A* **25**, 1211 (1969).
- ⁷⁰C. A. Pinkham and S. C. Wait, *J. Mol. Spectrosc.* **27**, 326 (1968).
- ⁷¹M. Wewer and F. Stienkemeier, *J. Chem. Phys.* **120**, 1239 (2004).
- ⁷²C. Bulliard, M. Allan, and S. Leach, *Chem. Phys. Lett.* **209**, 434 (1993).
- ⁷³L. Edwards, D. H. Dolphin, M. Gouterman, and A. D. Adler, *J. Mol. Spectrosc.* **38**, 16 (1971).
- ⁷⁴L. Edwards and M. Gouterman, *J. Mol. Spectrosc.* **33**, 292 (1970).
- ⁷⁵T. Stein, L. Kronik, and R. Baer, *J. Chem. Phys.* **131**, 244119 (2009).
- ⁷⁶T. Stein, L. Kronik, and R. Baer, *J. Am. Chem. Soc.* **131**, 2818 (2009).
- ⁷⁷A. Karolewski, T. Stein, R. Baer, and S. Kümmel, *J. Chem. Phys.* **134**, 151101 (2011).
- ⁷⁸A. Seidl, A. Görling, P. Vogl, J. A. Majewski, and M. Levy, *Phys. Rev. B* **53**, 3764 (1996).
- ⁷⁹R. Baer, E. Livshits, and U. Salzner, *Annu. Rev. Phys. Chem.* **61**, 85 (2010).
- ⁸⁰H. R. Eisenberg and R. Baer, *Phys. Chem. Chem. Phys.* **11**, 4674 (2009).